



Published in final edited form as:

*J Theor Biol.* 2015 December 07; 386: 177–187. doi:10.1016/j.jtbi.2015.09.006.

## An elaboration of theory about preventing outbreaks in homogeneous populations to include heterogeneity or preferential mixing

Zhilan Feng<sup>1</sup>, Andrew N. Hill<sup>2</sup>, Philip J. Smith<sup>3</sup>, and John W. Glasser<sup>3</sup>

<sup>1</sup>Department of Mathematics, Purdue University, West Lafayette, Indiana

<sup>2</sup>National Center for HIV/AIDS, Viral Hepatitis, STD, and TB Prevention, CDC, Atlanta, Georgia

<sup>3</sup>National Center for Immunization and Respiratory Diseases, CDC, Atlanta, Georgia

### Abstract

The goal of many vaccination programs is to attain the population immunity above which pathogens introduced by infectious people (e.g., travelers from endemic areas) will not cause outbreaks. Using a simple meta-population model, we demonstrate that, if sub-populations either differ in characteristics affecting their basic reproduction numbers or if their members mix preferentially, weighted average sub-population immunities cannot be compared with the proportionally-mixing homogeneous population-immunity threshold, as public health practitioners are wont to do. Then we review the effect of heterogeneity in average *per capita* contact rates on the basic meta-population reproduction number. To the extent that population density affects contacts, for example, rates might differ in urban and rural sub-populations. Other differences among sub-populations in characteristics affecting their basic reproduction numbers would contribute similarly. In agreement with more recent results, we show that heterogeneous preferential mixing among sub-populations increases the basic meta-population reproduction number more than homogeneous preferential mixing does. Next we refine earlier results on the effects of heterogeneity in sub-population immunities and preferential mixing on the effective meta-population reproduction number. Finally, we propose the vector of partial derivatives of the reproduction number with respect to the sub-population immunities as a fundamentally new tool for targeting vaccination efforts.

### Keywords

heterogeneity; population-immunity threshold; vaccine coverage

---

Correspondence: Dr. John Glasser; 1600 Clifton Road, NE; Mail Stop A-34; Atlanta, GA 30333 USA; +1-404-639-8780 (voice); +1-404-315-2493 (facsimile); jglasser@cdc.gov.

Contributions: ZF and AH performed the analyses and critiqued earlier drafts of the manuscript, JG conceived the study and wrote the manuscript, PS estimated vaccine coverage from National Immunization Surveys and critiqued earlier drafts of the manuscript. All authors have approved submission of this draft.

Conflicts: The authors declare that they have no conflicts of interest.

Disclaimer: The findings and conclusions in this report are those of the authors and do not necessarily represent the official position of the Centers for Disease Control and Prevention or other institutions with which they are affiliated.

## 1. Introduction

Human populations are heterogeneous, but all differences need not be modeled to answer any specific question. Immunity to vaccine-preventable diseases, for example, is heterogeneous within the United States (figures 1). Can differences among and within states be ignored in establishing vaccination coverage targets or monitoring progress in attaining them? The function used routinely for that purpose, the population-immunity threshold, involves the basic reproduction number, denoted  $\mathcal{R}_0$ . As this quantity is derived from a mathematical model, ascertaining its adequacy amounts to determining if the model from which it was derived is sufficiently detailed.

Mechanistic models are hypotheses about processes underlying natural phenomena. Simplicity is a virtue because it facilitates their evaluation. But the only way to ensure that one's model is not too simple is to compare results with those from models that include additional details that might affect them. In transmission modeling, one generally distinguishes sub-populations whose members have characteristics with which their risks of being infected or infecting others vary (e.g., age, gender, location). Levins (1) coined the term meta-population for any population whose members could be so stratified, although his own applications involved spatially-stratified populations.

Recently, Ball et al. (2) noted that the meta-population framework may preserve analytic tractability, unlike alternative means of incorporating salient structural heterogeneity, namely agent-based or network models. But they describe several challenges for modelers, among them clarifying the usefulness and limitations of systems of weakly coupled large sub-populations in modeling the spread of infections. Coupling strength determines a continuum whose limiting meta-populations behave as one or as multiple independent sub-populations. Here we endeavor to consolidate and extend the contributions of others who have considered intermediate situations.

Rates of person-to-person contact may vary with population density (e.g., be greater in urban than rural areas). They may also vary with personal characteristics (e.g., be greater among schoolchildren than younger and older people). The effect of such heterogeneity on  $\mathcal{R}_0$ , defined as the average number of secondary infections caused by a newly infectious person on introduction to a wholly susceptible population, was studied by Dietz (3), Anderson et al. (4), May and Anderson (5), and Diekmann et al. (6). These authors showed that, when mixing among sub-populations is proportional,  $\mathcal{R}_0$  varies with the contact rate's variance and mean.

Nold (7) developed a more general mixing framework in which a fraction of one's contacts is reserved for members of one's own group and the complement is distributed proportionately among groups. Jacquez et al. (8) allowed this fraction to vary among groups. Barbour (9), Dye and Hasibeder (10), Hasibeder and Dye (11), and Adler (12) showed that  $\mathcal{R}_0$  attains its maximum when individuals having high average *per capita* contact rates mix exclusively with each other.

May and Anderson (13, 14), Hethcote (15), and Hethcote and van Ark (16) considered heterogeneity in immunity. They concluded that the immunity above which newly

introduced infectious persons would not cause outbreaks, to which we refer as the naïve population-immunity threshold, was greater in heterogeneous populations than apparent if homogeneity was incorrectly assumed. But Hethcote and van Ark argued that the difference was modest if transmission rates were not too dissimilar. None of these authors considered preferential mixing.

Recently, Fine et al. (17) reviewed the history and applications of the population-immunity threshold,<sup>1</sup> which was derived from a model of a proportionally-mixing homogeneous population. In the next section, we define a meta-population model and mixing function with which to evaluate the utility of this threshold when mixing is preferential or sub-populations are heterogeneous with respect to characteristics affecting their basic reproduction numbers.

## 2. Methods

We employ the simplest meta-population model capable of informing vaccination policy to illustrate the effects of heterogeneity in sub-population contact rates and immunities, together with preferential mixing, on the effective reproduction number. A glossary accompanies this section.

Our model comprises  $n$  sub-populations in which people are susceptible,  $S_i$ , infected and infectious,  $I_i$ , or removed,  $R_i$  (from the infection process by virtue of immunization or immunity following infection),  $\mu$  is both the birth and death rate (introducing susceptible people without changing population size),  $p_i$  are proportions immunized at birth,  $\lambda_i$  are *per capita* forces (or hazard rates) of infection among susceptible people, and  $\gamma$  is the recovery rate. The rates  $\mu$  and  $\gamma$  are the reciprocals of life expectancy and the mean infectious period, respectively.

$$\begin{aligned}\frac{dS_i}{dt} &= \mu N_i(1 - p_i) - (\lambda_i + \mu)S_i \\ \frac{dI_i}{dt} &= \lambda_i S_i - (\gamma + \mu)I_i, \\ \frac{dR_i}{dt} &= \mu N_i p_i + \gamma I_i - \mu R_i, \\ N_i &= S_i + I_i + R_i, \quad i=1, \dots, n\end{aligned}$$

The force of infection among susceptible members of sub-population  $i$ ,

$\lambda_i := a_i \beta \sum_{j=1}^n c_{ij} (I_j/N_j)$ , where  $\beta$  is the probability of infection upon contacting an infectious person,  $a_i$  is the average contact rate in sub-population  $i$  (activity henceforth),  $c_{ij}$  is the proportion of the  $i^{\text{th}}$  sub-population's contacts that are with members of the  $j^{\text{th}}$  sub-population,  $I_j/N_j$  is the probability that a proportionally encountered member of sub-population  $j$  is infectious, and  $n$  is the number of sub-populations.

We follow Jacquez et al. (8), who modeled contacts among sub-populations (mixing henceforth) as  $c_{ij} := \varepsilon_j \delta_{ij} + (1 - \varepsilon_j) f_j$ , where  $f_j = (1 - \varepsilon_j) a_j N_j / \sum_{k=1}^n (1 - \varepsilon_k) a_k N_k$ ,  $\varepsilon_j$  is the fraction of their contacts that members of the  $j^{\text{th}}$  sub-population reserve for others in sub-

<sup>1</sup>We reserve the term “herd immunity” for the indirect effect of vaccination, a reduction in the force of infection experienced by unvaccinated members of a population by virtue of the vaccination of others.

population  $i$  (preference henceforth), and  $\delta_{ij}$  is the Kronecker delta, taking value 1 when  $i=j$  and 0 otherwise. Thus, the complement of  $\epsilon_i$  is distributed among all sub-populations including  $i$  in proportion to  $f_j$ , which describes activity-weighted proportional mixing. Jacquez et al. used this model for groups differing in sexual activity, but sub-population members could differ in age, location (e.g., reside in different households, in a city or surrounding villages), gender, or other discrete characteristics.

We limit  $n=2$  for transparency (i.e., analytical solutions are unwieldy, if possible to obtain, and graphing meta-population reproduction numbers or functions thereof against sub-population immunities, as we do in figures 2-8, is difficult when  $n>2$ ), but such calculations may be performed for any  $n$ . Indeed, the motivating application for this review and refinement of theoretical results is an assessment of vaccination among children attending elementary schools,<sup>2</sup> where  $n=200$  in the largest school district and  $n=638$  in the entire county. In such applications, effects that are modest when  $n=2$  become substantial.

For ease of reference, we define several terms based on the properties of  $(\epsilon_1, \epsilon_2, \dots, \epsilon_n)$ :

- i. Mixing is *proportional* if  $\epsilon_i = 0$  for all  $i$  (i.e., contacts are proportional to  $f_i$  a function described above).
- ii. Mixing is *preferential* if  $0 < \epsilon_i < 1$  for some  $i$  (i.e., a fraction  $\epsilon_i$  of the contacts of members of sub-population  $i$  are with others in their own sub-population and its complement is distributed proportionally among all sub-populations).
- iii. The  $i^{\text{th}}$  sub-population is *isolated* (i.e., members mix only with others in their own sub-population) if  $\epsilon_i = 1$ .
- iv. The *preferential* mixing is *homogeneous* if  $\epsilon_i = \epsilon$  for all  $i$ .
- v. The *preferential* mixing is *heterogeneous* if  $\epsilon_i \neq \epsilon_j$  for some  $i \neq j$ .

### 3. Results

First we derive the reproduction numbers for our model meta-population, whose sub-populations may differ in subscripted variables (numbers susceptible, infectious and recovered; proportions vaccinated at birth; contact rates and fractions within and among groups). Consequently, our model is more general than that of Goldstein et al. (18), whose households are populated by different numbers of identical individuals. Then we explore the impact of heterogeneity in activity,  $a_i$ , and immunity,  $p_i$ , on these numbers. Finally, we explore the interplay between such heterogeneity and preferential mixing (some  $\epsilon_i > 0$ ).

#### 3.1 Reproduction Numbers

In our model, the basic and effective reproduction numbers for sub-population  $i$ , denoted  $\mathcal{R}_{0i}$  and  $\mathcal{R}_{vi}$ , respectively, which differ by vaccination as denoted by subscript  $v$ , are

<sup>2</sup>In the United States, elementary schools are located in the neighborhoods where most of their students reside. Thus, neighborhoods are the smallest sub-populations for which immunity to specific vaccine-preventable diseases can be calculated from proportions vaccinated, routinely surveyed at school-entry and exit, and vaccine efficacy.

$$R_{0i} = \frac{\beta a_i}{\gamma + \mu}, R_{vi} = R_{0i}(1 - p_i).$$

Meta-population reproduction numbers are properties of next-generation matrices (19, 20) that translate vectors composed of the numbers infectious in each sub-population at one time (e.g., outbreak generation) into the corresponding vectors at other times (or generations). The largest eigenvalue is the average factor by which successive vectors differ in magnitude, or average number of secondary infections per infectious person, at equilibrium.

We derive the next-generation matrix  $K$  for the simplest meta-population (with  $n = 2$ ) in appendix 1 (and, to dispel the notion that this somehow limits the generality of our

arguments,  $n = 3$  in appendix 2). When  $n = 2$ ,  $K = \begin{bmatrix} R_{v1}c_{11} & R_{v1}c_{12} \\ R_{v2}c_{21} & R_{v2}c_{22} \end{bmatrix}$ , whose larger eigenvalue,

$$R_v = \frac{1}{2} [A + D + \sqrt{(A - D)^2 + 4BC}],$$

where  $A = R_{v1}c_{11}$ ,  $B = R_{v1}c_{12}$ ,  $C = R_{v2}c_{21}$ ,  $D = R_{v2}c_{22}$ . If  $0 < \bar{e} < 1$ , one cannot generally write explicit expressions for the meta-population  $\mathfrak{R}_v$  when  $n > 4$ , but can always compute it numerically. The contributions of sub-population characteristics and preferential mixing that are described in the following sections depend on the structure of the next-generation matrix  $K$ , which could be written as the product of a diagonal matrix whose elements are  $\mathfrak{R}_{vi}$  and matrix whose elements are  $c_{ij}$ .

### 3.2 Population Heterogeneity

As shown originally by Dietz (3), and subsequently by Anderson et al. (4), May and Anderson (5), and Diekmann et al. (6), when mixing is proportional, the basic reproduction number can also be written as

$$\mathfrak{R}_0 = \bar{\mathfrak{R}}_0 + \frac{\beta}{\gamma + \mu} \times \frac{\sigma^2}{m},$$

where  $\bar{\mathfrak{R}}_0$  is the mean  $\mathfrak{R}_0$ , and  $m$  and  $\sigma^2$  are the mean and variance of activity among sub-populations. We observe that similar expressions could be derived for any characteristic affecting  $\mathfrak{R}_0$ . The probability of infection on contact with an infectious person might reflect age-specific differences in susceptibility,  $\beta_i$  for one example, or the recovery rate reflect location-specific differences in medical care,  $\gamma_i$  for another.

We find the spectral radius (eigenvalue of greatest magnitude) of the matrix  $K$  more intuitive because it generalizes easily to preferential mixing. But we derive this classic result mostly to demonstrate that such heterogeneity increases  $\mathfrak{R}_0$  even when mixing is proportional, and

also because some of its many variations are incorrect. We also provide an example where two meta-populations have the same mean activity, but differ in their variances. In table 1, heterogeneity in sub-population activities increases  $\mathfrak{R}_0$  from 3.50 to 3.72 for proportional mixing ( $\varepsilon_1 = \varepsilon_2 = 0$ ) and preferential mixing ( $\varepsilon_1 = \varepsilon_2 = 0.5$ ) further increases it to 3.88. Evidently preferential mixing magnifies the effect of heterogeneity in activity, one sub-population characteristic affecting  $\mathfrak{R}_{0j}$  in our simple meta-population model.

Figure 2 complements the empirical analyses tabulated, showing how heterogeneity in preference, another sub-population characteristic affecting  $\mathfrak{R}_{0j}$ , modifies the effect of heterogeneity in activity. Consider the case when  $n = 2$  with fixed total activity  $a_T := a_1 + a_2$ , and all other parameters identical for the two sub-populations except  $\varepsilon_j$ . In appendix 3, we show that:

- i. for  $\varepsilon_1 = \varepsilon_2 = 0$ ,  $\mathfrak{R}_0(0, 0)$  is minimized when  $a_1 = a_2 = a_T/2$  and is a monotonically increasing function of the difference  $|a_2 - a_1|$  (i.e.,  $\mathfrak{R}_0$  is maximized when heterogeneity in activity is greatest);
- ii. a similar result as in (i) holds when either  $\varepsilon_1 = 1$  or  $\varepsilon_2 = 1$ . That is,  $\mathfrak{R}_0(\varepsilon_1, 1) = \mathfrak{R}_0(1, \varepsilon_2)$  as shown in appendix 3. This is minimized when  $a_1 = a_2 = a_T/2$  and is a monotonically increasing function of the difference  $|a_2 - a_1|$ . Therefore,  $\mathfrak{R}_0(\varepsilon_1, 1) = \mathfrak{R}_0(1, \varepsilon_2)$  is maximized when heterogeneity in activity is greatest.

### 3.3 Mixing among Sub-Populations

Preference, the fraction of contacts reserved for one's own sub-population, ranges over the unit interval, but we can derive explicit limiting conditions (i.e.,  $\varepsilon = 0$ ,  $\varepsilon = 1$ ) from our equations for the meta-population reproduction numbers when  $n = 2$ .

Case 1 (isolated sub-populations): When  $\varepsilon_1 = \varepsilon_2 = 1$ , we have  $c_{11} = 1$ ,  $c_{12} = 0$ ,  $c_{21} = 0$ ,  $c_{22} = 1$ . Thus, in the expression above for the largest eigenvalue of the next-generation matrix  $K$ ,

$$A=R_{v1}, B=0, C=0, D=R_{v2}, \text{ and} \\ R_v = \frac{1}{2} [R_{v1} + R_{v2} + \sqrt{(R_{v1} - R_{v2})^2}] = \begin{cases} \frac{1}{2} [R_{v1} + R_{v2} + R_{v1} - R_{v2}] = R_{v1}, & \text{if } R_{v1} > R_{v2} \\ \frac{1}{2} [R_{v1} + R_{v2} + R_{v2} - R_{v1}] = R_{v2}, & \text{if } R_{v1} < R_{v2} \end{cases}.$$

That is,  $R_v = \max\{R_{v1}, R_{v2}\}$ . When  $p_1 = p_2 = 0$ , we have  $\mathfrak{R}_{vi} = \mathfrak{R}_{0i}$  whereupon  $R_0 = \max\{R_{01}, R_{02}\}$ .

Case 2 (proportionally mixing sub-populations): When  $\varepsilon_1 = \varepsilon_2 = 0$ , we have  $c_{11} = f_1$ ,  $c_{12} = f_2$ ,  $c_{21} = f_1$ ,  $c_{22} = f_2$ . Thus,  $A = R_{v1} f_1$ ,  $B = R_{v1} f_2$ ,  $C = R_{v2} f_1$ ,  $D = R_{v2} f_2$ , and

$$R_v = \frac{1}{2} [R_{v1}f_1 + R_{v2}f_2 + \sqrt{(R_{v1}f_1 - R_{v2}f_2)^2 + 4R_{v1}f_2R_{v2}f_1}] = \frac{1}{2} [R_{v1}f_1 + R_{v2}f_2 + \sqrt{(R_{v1}f_1 + R_{v2}f_2)^2}] = R_{v1}f_1 + R_{v2}f_2.$$

When  $p_1 = p_2 = 0$ , we have  $\mathfrak{R}_{vi} = \mathfrak{R}_{0i}$ , whereupon  $R_0 = R_{01}f_1 + R_{02}f_2$ . Chow et al. (21, Section 3.1) proved that  $\mathfrak{R}_v / \varepsilon_i > 0$  ( $i = 1, 2$ ) for all  $0 < \varepsilon_i < 1$ , affirming earlier conjectures (8-11).

Goldstein et al. (18) define several reproduction numbers, among them the average number of infections in other households caused by an infected member of an index household. If we consider our meta-population  $\mathfrak{R}_v = \mathfrak{R}_v(\varepsilon_1, \varepsilon_2)$  as a function of  $\varepsilon_1$  and  $\varepsilon_2$ , we can solve for the critical value of  $\varepsilon_{1c}$  at which  $\mathfrak{R}_v(\varepsilon_{1c}, \varepsilon_2) = 1$  for any given value of  $\varepsilon_2$ . Recall that

$$R_v = \frac{1}{2} [A + D + \sqrt{(A - D)^2 + 4BC}],$$

where  $A(\varepsilon_1, \varepsilon_2) = R_{v1}c_{11}$ ,  $B(\varepsilon_1, \varepsilon_2) = R_{v1}c_{12}$ ,  $C(\varepsilon_1, \varepsilon_2) = R_{v2}c_{21}$ ,  $D(\varepsilon_1, \varepsilon_2) = R_{v2}c_{22}$  with

$$c_{11} = \varepsilon_1 + \frac{(1-\varepsilon_1)^2 a_1 N_1}{(1-\varepsilon_1)a_1 N_1 + (1-\varepsilon_2)a_2 N_2}, \quad c_{12} = \frac{(1-\varepsilon_1)(1-\varepsilon_2)a_2 N_2}{(1-\varepsilon_1)a_1 N_1 + (1-\varepsilon_2)a_2 N_2},$$

$$c_{21} = \frac{(1-\varepsilon_1)(1-\varepsilon_2)a_1 N_1}{(1-\varepsilon_1)a_1 N_1 + (1-\varepsilon_2)a_2 N_2}, \quad c_{22} = \varepsilon_2 + \frac{(1-\varepsilon_2)^2 a_2 N_2}{(1-\varepsilon_1)a_1 N_1 + (1-\varepsilon_2)a_2 N_2}.$$

Note that  $\mathfrak{R}_v(\varepsilon_1, \varepsilon_2)$  is an increasing function of  $\varepsilon_1$  (21). Hence, if  $\mathfrak{R}_v(0, \varepsilon_2) > 1$ , then  $\mathfrak{R}_v(\varepsilon_1, \varepsilon_2) > 1$  for all  $\varepsilon_1$ . If  $\mathfrak{R}_v(0, \varepsilon_2) < 1$ , however, we can solve the equation  $\mathfrak{R}_v(\varepsilon_1, \varepsilon_2) = 1$  for  $\varepsilon_1$  and arrive at

$$\varepsilon_{1c} = \frac{a_1 N_1 (R_{v1} - 1)(1 - R_{v2} \varepsilon_2) + a_2 N_2 (R_{v2} - 1)(1 - \varepsilon_2)}{a_1 N_1 (R_{v1} - 1)(1 - R_{v2} \varepsilon_2) + a_2 N_2 R_{v1} (R_{v2} - 1)(1 - \varepsilon_2)}.$$

This expression provides a formula for  $\varepsilon_{1c}$  that is feasible if and only if the other parameter values are such that  $0 < \varepsilon_{1c} < 1$ . Thus,  $\varepsilon_{1c}$  provides a critical value for  $\mathfrak{R}_v = 1$ . This formula holds if  $\mathfrak{R}_v$  is replaced by  $\mathfrak{R}_0$  (with  $\mathfrak{R}_{vi}$  being replaced by  $\mathfrak{R}_{0i}$ ) as long as  $\mathfrak{R}_0(0, \varepsilon_2) < 1$ .

### 3.4 Heterogeneous Preferential Mixing

Colizza and Vespignani (22) note that heterogeneity in connectivity, by which they represent individual movement in a spatial meta-population, increases the reproduction number. While our meta-population need not be spatial, distributing the  $1 - \varepsilon_j$  contacts not reserved for members of sub-population  $i$  generally requires movement. Returning to table 1, we see that while preferential mixing ( $\varepsilon_j = \varepsilon_2 = 0.5$ ) among sub-populations differing in  $\mathfrak{R}_{0i}$  increases



the meta-population  $\mathfrak{R}_0$  compared to proportional mixing ( $\varepsilon_1 = \varepsilon_2 = 0$ ), heterogeneous preferential mixing ( $\varepsilon_1 = 0.25, \varepsilon_2 = 0.75$  or vice versa) increases  $\mathfrak{R}_0$  compared to homogeneous preferential mixing (from 3.88 to 3.92 or 3.98). When  $n = 2$ , if either sub-population is isolated ( $\varepsilon_1 = 0, \varepsilon_2 = 1$  or vice versa), both are isolated (appendix 3), whereupon  $\mathfrak{R}_0 = \max\{\mathfrak{R}_{01}, \mathfrak{R}_{02}\} = 4.37$  as noted in the previous section. Apolloni et al. (23) consider social as well as spatial strata, neither however differing in as many respects as sub-populations in our single stratification. Comparable results are similar, affirming our conclusion that differences among sub-populations in factors affecting their reproduction numbers matter, not the means by which such heterogeneity arises.

### 3.5 Heterogeneity in Immunity

Figures 3 illustrate the impact of heterogeneity in  $p_i$  on  $\mathfrak{R}_v$  in meta-populations whose sub-populations are the same size (scenario B of table 1), but mix proportionally and preferentially on the left and right, respectively. Heterogeneity increases away from the line of equality connecting the points at which  $(p_1, p_2) = 0$  and  $(p_1, p_2) = 1$ . Values of  $\mathfrak{R}_v$  for all combinations of  $p_i (i = 1, 2)$  form a plane when mixing is proportional, but curve upward about the above-mentioned line when mixing is preferential. Values at or below their intersection with the dark blue plane,  $\mathfrak{R}_v = 1$ , are combinations of  $p_i (i = 1, 2)$  at which population-immunity attains or exceeds this threshold.

Because mixing affects  $\mathfrak{R}_v$ , the impact of heterogeneity in  $p$  cannot be assessed absent information about mixing. Setting  $\varepsilon_1 = \varepsilon_2 = \varepsilon$ , for example, we observe that for fixed  $0 < \varepsilon < 1$  a curve in the  $p_1$ - $p_2$  plane divides the region  $0 \leq p_1 \leq 1, 0 \leq p_2 \leq 1$  into sub-regions such that  $\mathfrak{R}_v > 1 (< 1)$  for  $(p_1, p_2)$  below (above) the curve (figures 4). Moreover, the area below (above) the curve increases (decreases) as  $\varepsilon$  increases. This suggests that the more preferentially sub-populations mix (higher  $\varepsilon$ ), the more difficult outbreak prevention becomes (i.e., the greater the requisite values of  $\bar{p}$ ).

When  $\varepsilon = 0$  and  $\varepsilon = 1$ , the regions in which  $\mathfrak{R}_v > 1$  and  $\mathfrak{R}_v < 1$  are a (possibly truncated) triangle and rectangle, respectively. The shapes of these regions depend on whether sub-populations are isolated ( $\varepsilon = 1$ ), in which case the threshold immunities are independent (and thus horizontal or vertical lines), or their members mix proportionally ( $\varepsilon = 0$ ), in which case the meta-population threshold depends on the immunity levels of both sub-populations (and thus a line that is neither horizontal nor vertical). The slope of this line depends on the values of parameters affecting  $\mathfrak{R}_{0i}$ , the average contact rate or activity ( $a_1$  and  $a_2$ ) in our meta-population model. Vaccinating the sub-population whose members have higher *per capita* contact rates would more effectively reduce  $\mathfrak{R}_v$ .

There is one exception. The curves intersect the straight line in figures 4 at the point  $(1 - 1/\mathfrak{R}_{01}, 1 - 1/\mathfrak{R}_{02})$ , at which  $\mathfrak{R}_{v1} = \mathfrak{R}_{v2} = 1$ , whereupon the next-generation matrix

$$K_v = \begin{bmatrix} \mathfrak{R}_{v1} & 0 \\ 0 & \mathfrak{R}_{v2} \end{bmatrix} \begin{bmatrix} c_{11} & c_{12} \\ c_{21} & c_{22} \end{bmatrix} = \begin{bmatrix} c_{11} & c_{12} \\ c_{21} & c_{22} \end{bmatrix},$$



whose dominant eigenvalue is  $1 \forall \epsilon$ .

Using a model meta-population composed of a city and several villages, May and Anderson (13, 14) showed that heterogeneity in relevant sub-population characteristics also increased  $\mathcal{R}_v$ . Hethcote and van Ark (16) argued that person-to-person contact rates in densely-populated urban areas should be no more than twice those in sparsely-populated rural ones. This change in parameter values diminished the apparent effect of heterogeneity. Our more transparent example (table 2) demonstrates that the effect on  $\mathcal{R}_0$  (and, as  $\mathcal{R}_v$  is a function of  $\mathcal{R}_0$ , on  $\mathcal{R}_v$  as well) is greater when mixing is preferential ( $\epsilon_1 = \epsilon_2 \neq 0$ ) than proportional ( $\epsilon_1 = \epsilon_2 = 0$ ) if sub-population sizes are equal (e.g., both  $0.5N$ ). When 90% of the people are in one sub-population and 10% in another (e.g., a city and village), our results resemble Hethcote's and van Ark's.

In figures 5, we refine May's and Anderson's (13) conclusion that “under a uniformly applied immunization programme, the overall fraction that must be immunized is larger than would be estimated by (incorrectly) assuming the population to be homogeneously mixed.” Preferential mixing curves the level contours of  $\mathcal{R}_v$  in the  $p_1$ - $p_2$  plane that otherwise would be straight lines. Consequently, uniform immunization ( $p_1 = p_2$ ) of meta-populations composed of sub-populations that are identical in characteristics affecting  $\mathcal{R}_{0i}$  does indeed attain  $\mathcal{R}_v=1$  (or any other value) most efficiently. When sub-populations differ in such characteristics, however, this is no longer true (e.g., Keeling's and Rohani's (24) figure 3.3 resembles our figure 5b). In general, the optimal strategy vaccinates members of the sub-population whose  $\mathcal{R}_{0i}$  is greatest disproportionately.

Fine et al. (17) provide an example with  $n=2$  in which  $\mathcal{R}_{01} = 5$  and  $\mathcal{R}_{02} = 1$  and  $\mathcal{R}_0 = 5$ , so their sub-populations must be isolated (i.e.,  $\epsilon_1 = \epsilon_2 = 1$ , whereupon  $c_{12} = c_{21} = 0$ ). They state, “Because the high-risk group is responsible for any increase in incidence, outbreaks could in theory be prevented by vaccinating 80% of the high-risk group alone, thus,  $< 80\%$  of the entire population.” This is true, but only because their meta-population is composed of isolated sub-populations. Keeling and Rohani (24) state that “In structured models, the critical level of vaccination that eradicates infection is the same as in unstructured models,  $1 - 1/\mathcal{R}_0$ , if vaccination is applied at random,” which is true only if  $\mathcal{R}_0$  is correctly specified. And  $\mathcal{R}_0$  in structured and unstructured populations differ. Assuming, in the example of Fine et al., that  $\beta = 0.05$ ,  $\gamma = 0.15$ ,  $\mu = 0$  and that sub-population sizes are the same, we have  $a_1 = 15$  and  $a_2 = 3$ . Averaging these contact rates, which is tantamount to assuming a proportionally-mixing homogeneous population,  $\bar{a} = 9$ , whereupon  $\mathcal{R}_0 = 3$  and the naïve population-immunity threshold,  $p_c = 0.67$ . Contact heterogeneity ( $a_1 = 15$  and  $a_2 = 3$ ) increases  $\mathcal{R}_0$  to 4.3, while preferential mixing ( $\epsilon_1 = \epsilon_2 = 1$ ) further increases it to 5.

### 3.6 The Negative Gradient

Evidently  $\mathcal{R}_v$  depends not only on the immunity,  $p_i$  of sub-populations  $i$ , but also on the fractions of contacts,  $\epsilon_i$  that members reserve for others in their own sub-populations, and their proportional mixing functions,  $f_j$  which also depend on sub-population sizes,  $N_j$ , and *per capita* contact rates,  $a_j$ , which may be functions of density. We can assess how these various factors modify the effect of the  $p_i$  on  $\mathcal{R}_v$  via the gradient, the vector of partial derivatives of  $\mathcal{R}_v$  with respect to the  $p_i$ :

For any meta-population immunity  $(p_{1c}, p_{2c})$ , the gradient (a vector-valued function)

$\nabla \mathfrak{R}_v|_{(p_{1c}, p_{2c})} = \left( \frac{\partial \mathfrak{R}_v}{\partial p_1}, \frac{\partial \mathfrak{R}_v}{\partial p_2} \right)|_{(p_{1c}, p_{2c})}$  gives the direction (in the  $(p_1, p_2)$ -plane) along which the rate of change in  $\mathfrak{R}_v$  is greatest and has length equal to its rate of change in that direction. Furthermore, when  $p_{1c}$  and  $p_{2c}$  change by amounts  $a$  and  $b$  (assumed small and positive for our purposes), the corresponding change in  $\mathfrak{R}_v$ ,  $\mathfrak{R}_v$ , can be approximated by

$$\mathfrak{R}_v(p_{1c}+a, p_{2c}+b) - \mathfrak{R}_v(p_{1c}, p_{2c}) \approx \nabla \mathfrak{R}_v|_{(p_{1c}, p_{2c})} \cdot (a, b) = a \frac{\partial \mathfrak{R}_v}{\partial p_1}|_{(p_{1c}, p_{2c})} + b \frac{\partial \mathfrak{R}_v}{\partial p_2}|_{(p_{1c}, p_{2c})}.$$

A familiar analogy may clarify this concept: Consider a topographic map with elevations represented by contour lines and axes latitude and longitude. In the equation above,  $\mathfrak{R}_v$  is approximated by the dot product (the “ $\cdot$ ”) of  $\nabla \mathfrak{R}_v$  with the 2-D vector  $(a, b) = (p_1, p_2)$ . In our analogy, this vector equals  $(\text{lat}, \text{lon})$ . Our  $|\nabla \mathfrak{R}_v|$ , the length of the gradient vector, corresponds to the rate of change in elevation with distance. The direction of the negative gradient, orthogonal to the level surface at  $(p_1, p_2)$ , is that in which this rate of increase is greatest (i.e., the steepest route).

Chow et al. (21, Section 3.1) showed that  $\mathfrak{R}_v$  decreases with  $p_1$  and  $p_2$ . For example,

$$\frac{\partial \mathfrak{R}_v}{\partial p_1} = -\frac{1}{2} \left[ R_{01}c_{11} + R_{02}c_{22} + \frac{R_{v1}c_{11} + R_{01}R_{v2}(1 + c_{12}c_{21})}{\sqrt{(R_{v1}c_{11} - R_{v2}c_{22})^2 + 4R_{v1}R_{v2}c_{12}c_{21}}} \right] < 0,$$

and similarly,  $\partial \mathfrak{R}_v / \partial p_2 < 0$ . As increasing any element of a non-negative matrix decreases its dominant eigenvalue according to Perron-Frobenius theory, these partials are negative for arbitrary  $n$ . For any given point  $(p_{1c}, p_{2c})$ , we can use them to determine the joint changes in  $p_1$  and  $p_2$  for which the rate of change in  $\mathfrak{R}_v$  is greatest (figures 6).

### 3.7 Targeting Vaccination

The gradient provides a means of identifying which sub-population to vaccinate to affect  $\mathfrak{R}_v$  the most. Figure 6a illustrates the  $\mathfrak{R}_v$  corresponding to  $p_1$  and  $p_2$  of 5%. Figures 6b and c illustrate the magnitudes of the vector,  $\nabla \mathfrak{R}_v$  and directions of the negative gradient at each point, respectively. We observe that different trajectories follow the gradient depending on starting point. Near the point  $p_1 = 1$  and  $p_2 = 0$ , the arrow is almost vertical (i.e., the gradient direction has only a small  $p_1$  component), indicating that changes in  $p_2$  would affect  $\mathfrak{R}_v$  the most.

In the example of Fine et al. (17), sub-population contact rates different considerably. For illustrative purposes, let  $a_1 = 15$  and  $a_2 = 12$  so that  $\mathfrak{R}_{01} = 5$  and  $\mathfrak{R}_{02} = 4$  (the values of  $\beta$  and  $\gamma$  are the same as before, i.e.,  $\beta = 0.05$  and  $\gamma = 0.15$ ). If  $\varepsilon_1 = \varepsilon_2 = 1$ , then for all  $(p_1, p_2)$  with  $p_2 > (5/4)p_1 - 1/4$ , we have that  $\mathfrak{R}_v = \mathfrak{R}_{v1} = 5(1 - p_1)$ , which implies that the gradient direction is horizontal; thus, only population 1 need be vaccinated to attain  $\mathfrak{R}_v = 1$ .

However, this is true only when sub-populations are isolated. For example, let  $\varepsilon_1 = \varepsilon_2 = 0.3$ ,

$N_1 = 1100$ , and  $N_2 = 900$ . In this case, illustrated in figure 7a, we observe that the gradient is neither horizontal nor vertical for any  $(p_1, p_2)$ . We observe also that the trajectories in the  $p_1$ - $p_2$  plane, when the gradient direction is followed, are not straight lines, as shown in figure 7b. While this may be perfectly obvious when  $n = 2$ , meta-populations generally comprise many more or less interconnected sub-populations.

### 3.8 Optimal Vaccine Coverage

The gradient also describes the most efficient means of attaining any programmatic goal: To illustrate this, we fix  $\mathcal{R}_v$  (i.e., the amount by which  $\mathcal{R}_v$  is to be reduced). Without loss of generality, we assume that  $\mathcal{R}_v$  is small (or that the prescribed reduction of  $\mathcal{R}_v$  is a sum of small increments) and denote the gradient vector at the point  $(p_1, p_2)$  by  $\nabla \mathcal{R}_v = (v_1, v_2)$ .

If we increase the fractions immune by  $p_1$  and  $p_2$  along a unit direction,  $\vec{u} = (a, b)$ , then  $(p_1, p_2) = r\vec{u}$ , where  $r$  is a constant determining the magnitude of the vector  $(p_1, p_2)$ . It follows that  $\mathcal{R}_v \approx (v_1, v_2) \cdot (r\vec{u})$ , so that  $|\mathcal{R}_v| \approx r|(v_1, v_2)| \times |\cos \Theta|$ , where  $\Theta$  is the angle between the gradient vector at  $(p_1, p_2)$  and the unit length vector  $\vec{u}$ . Note that the expression  $|(v_1, v_2)| \times |\cos \Theta|$  is largest when  $|\cos \Theta| = 1$  (i.e., when  $\Theta = \pi$ , because  $\mathcal{R}_v / p_i < 0$ ). Thus, the value  $r$  is minimized when  $\vec{u}$  is parallel to the gradient vector  $(v_1, v_2)$ ; that is,  $\vec{u} = (v_1, v_2) / |(v_1, v_2)|$ . Thus,  $(p_1, p_2) \approx r(v_1, v_2) / |(v_1, v_2)|$ , whereupon  $p_1 N_1 + p_2 N_2 \approx r(v_1 N_1 + v_2 N_2) / |(v_1, v_2)|$ . Therefore, the increase in doses  $p_1 N_1 + p_2 N_2$  is smallest when the vector  $(p_1, p_2)$  is parallel to the gradient vector  $\nabla \mathcal{R}_v$  at the point  $(p_1, p_2)$ . Goldstein et al. (25) consider the similar problem of the  $\nabla \mathcal{R}_v$  that could be attained by optimally allocating a fixed amount of vaccine.

The gradient can also be used to devise optimal allocation strategies for limited vaccines. We can minimize  $\mathcal{R}_v(p_1, p_2)$  for fixed total vaccine doses  $p_1 N_1 + p_2 N_2 = c$ , where  $c > 0$  is a constant representing the doses available, with  $N_1$  and  $N_2$  being fixed constants. In this case, we solve the equation  $\nabla \mathcal{R}_v + \lambda(N_1, N_2) = 0$ , subject to  $p_1 N_1 + p_2 N_2 = c$ , where  $\lambda$  is the Lagrange multiplier. Notice that the constraint corresponds to a line whose equation is  $p_2 = (c - p_1 N_1) / N_2$ . As this line is orthogonal to  $\nabla \mathcal{R}_v$  at the solution point  $(p_1, p_2)$ , its intersection with the contour curve  $\mathcal{R}_v(p_1, p_2)$  to which it is tangent (figure 8) is the optimal vaccination program. Thus, for this set of parameter values and constraint,  $p_1 = 0.66$  and  $p_2 = 0.29$  reduces  $\mathcal{R}_0 = 4.6$  (when  $p_1 = p_2 = 0$ ) to  $\mathcal{R}_v \approx 2.2$ .

## 4. Discussion

Using the simplest meta-population model that is capable of informing vaccination policy, we reproduce earlier results concerning the effect of heterogeneity in inter-personal contact rates – attributable, for example, to disparate sub-population densities – on the basic meta-population reproduction number. We observe that this reasoning extends to any variable affecting sub-population reproduction numbers. Preferential mixing, especially if heterogeneous, also affects the basic meta-population reproduction number. We refine earlier results on effects of heterogeneity in sub-population immunities and preferential mixing on the effective meta-population reproduction number. Heterogeneity in immunity can result from disparate socioeconomic circumstances, religious or philosophical beliefs, or information about the risks and benefits of vaccination, to name but a few possible causes.

## 4.1 Theory

Were populations proportionally-mixing or homogeneous, the population-immunity threshold would inform vaccination programs to mitigate the risk of outbreaks upon the introduction of infectious people. For diseases that had been eliminated domestically, these would be travelers infected abroad. This threshold is defined as the immunity at which an average infectious person infects only one susceptible person.

If individuals differed only in the sizes of their sub-populations, one could use the meta-population reproduction number to determine a single population-immunity threshold, as Goldstein et al. (18) do on their page 20. But, when populations are either heterogeneous in characteristics affecting basic reproduction numbers (glossary,  $\mathcal{R}_0$ ) or sub-population members mix preferentially (glossary,  $0 < \epsilon_j < 1$ ), sets of sub-population immunities (i.e., pairs if there are only two sub-populations, triplets if there are three, and so on) satisfy the condition that only one susceptible person is infected per infectious person. Unless sub-populations are identical in characteristics affecting their basic reproduction numbers and their members mix proportionally, these sets cannot simply be averaged for comparison with overall or weighted average sub-population immunities, as is current public health practice.

Meta-population reproduction numbers (glossary,  $\mathcal{R}_0, \mathcal{R}_v$ ) account for heterogeneity and preferential mixing, inevitable in spatial meta-populations inasmuch as proximity affects contacts. If effective meta-population reproduction numbers – average numbers of secondary infections per infectious person – exceed, equal or are less than one, the numbers of infected people will increase, remain the same, or diminish, respectively. Thus, vaccination programs designed to mitigate the risk of outbreaks should maintain effective meta-population reproduction numbers less than one.

## 4.1 Practice

Our first result of programmatic import is that, in assessing the impact of heterogeneity, one cannot ignore mixing. Mixing not only modifies the effects of heterogeneity, but identifies relevant sub-populations (i.e., mixing is proportional within and preferential between them). While others have recognized its importance (9-12), mixing has only recently begun being measured (26-28). However, geospatial location devices and proximity detectors promise to dramatically increase our understanding of the contact patterns by which the pathogens causing infectious diseases in host meta-populations are transmitted.

Our second such result is that differences among sub-populations in characteristics affecting their basic reproduction numbers – heterogeneity – may substantially increase meta-population reproduction numbers, especially when combined with preferential mixing. Sub-population members can differ, but not in these characteristics. We began by questioning whether sub-populations themselves were needed. In reaching this conclusion, we extend the contributions of many authors, some of whom studied characteristics affecting basic reproduction numbers (3-6) and others immunity (13-16), the additional characteristic affecting effective reproduction numbers.

Our third result of programmatic import is the gradient, a fundamentally new tool for exploring the combined effects of heterogeneity in characteristics affecting sub-population

reproduction numbers and mixing among the members of different sub-populations on the average number of secondary infections per infectious person. The gradient evaluated at the point  $(p_1, \dots, p_n)$  is a vector giving the direction in which to move away from  $(p_1, \dots, p_n)$  so as to achieve the greatest change in  $\mathfrak{R}_v$ .

We demonstrate that, at any point in the  $n$ -dimensional space described by sub-population immunities, increasing them in direction of the negative gradient would most efficiently (i.e., use the fewest doses of vaccine) achieve any desired reduction in the average number of secondary infections per infectious person. This belies Keeling's and Rohani's (24) assertion that "only for the very simplest of models can the calculation of optimal targeting be performed analytically," providing an alternative to Medlock and Galvani's (29) simulation of an age-structured population model with different vaccine allocations and comparison of cases or death averted.

## Acknowledgments

We are grateful to Lance Rodewald for suggesting that the impact of heterogeneity in vaccine coverage on the population-immunity threshold might be amenable to modeling, to Dan Higgins for improving our illustrations, and to Aaron Curns and several anonymous reviewers for constructively critiquing earlier drafts of the manuscript.

Funding: ZF's research is supported in part by NSF grant DMS-1022758.

## Appendix 1

Given that  $N = S + I + R$ , we can eliminate one equation.

Letting

$$\begin{aligned} x_i &= \frac{S_i}{N_i}, \quad y_i = \frac{I_i}{N_i}, \quad i=1, 2 \\ x_1' &= \mu(1-p_1) - (\lambda_1 + \mu)x_1 \\ x_2' &= \mu(1-p_2) - (\lambda_2 + \mu)x_2 \\ y_1' &= \lambda_1 x_1 - (\gamma + \mu)y_1 \\ y_2' &= \lambda_2 x_2 - (\gamma + \mu)y_2 \\ \lambda_i &= a_i \beta \sum_j c_{ij} y_j \end{aligned}$$

At the disease-free equilibrium,  $x_i = 1 - p_i$ ,  $i = 1, 2$

Substituting,

$$\begin{aligned} y_1' &= (a_1 c_{11} \beta y_1 + a_1 c_{12} \beta y_2)(1 - p_1) - (\gamma + \mu)y_1 = f_1(y_1, y_2) \\ y_2' &= (a_2 c_{21} \beta y_1 + a_2 c_{22} \beta y_2)(1 - p_2) - (\gamma + \mu)y_2 = f_2(y_1, y_2) \end{aligned}$$

The Jacobian,

$$J = \begin{pmatrix} \frac{\partial f_1}{\partial y_1} & \frac{\partial f_1}{\partial y_2} \\ \frac{\partial f_2}{\partial y_1} & \frac{\partial f_2}{\partial y_2} \end{pmatrix}_{(y_1=0, y_2=0)} = \begin{pmatrix} a_1 c_{11} \beta (1 - p_1) - (\gamma + \mu) & a_1 c_{12} \beta (1 - p_1) \\ a_2 c_{21} \beta (1 - p_2) & a_2 c_{22} \beta (1 - p_2) - (\gamma + \mu) \end{pmatrix}$$

We can rewrite  $J$  as  $FV$ , where  $F$  are infection and  $V$  other terms

$$J = \begin{pmatrix} a_1 c_{11} \beta (1 - p_1) & a_1 c_{12} \beta (1 - p_1) \\ a_2 c_{21} \beta (1 - p_2) & a_2 c_{22} \beta (1 - p_2) \end{pmatrix} - \begin{pmatrix} (\gamma + \mu) & 0 \\ 0 & (\gamma + \mu) \end{pmatrix}$$

The next-generation matrix  $K = FV^{-1}$

$$\begin{aligned} K &= \begin{pmatrix} a_1 c_{11} \beta (1 - p_1) & a_1 c_{12} \beta (1 - p_1) \\ a_2 c_{21} \beta (1 - p_2) & a_2 c_{22} \beta (1 - p_2) \end{pmatrix} \\ &\quad \times \begin{pmatrix} \frac{1}{(\gamma + \mu)} & 0 \\ 0 & \frac{1}{(\gamma + \mu)} \end{pmatrix} \\ &= \begin{pmatrix} \frac{a_1 c_{11} \beta (1 - p_1)}{(\gamma + \mu)} & \frac{a_1 c_{12} \beta (1 - p_1)}{(\gamma + \mu)} \\ \frac{a_2 c_{21} \beta (1 - p_2)}{(\gamma + \mu)} & \frac{a_2 c_{22} \beta (1 - p_2)}{(\gamma + \mu)} \end{pmatrix} \\ &= \begin{pmatrix} \mathfrak{R}_{01} (1 - p_1) c_{11} & \mathfrak{R}_{01} (1 - p_1) c_{12} \\ \mathfrak{R}_{02} (1 - p_2) c_{21} & \mathfrak{R}_{02} (1 - p_2) c_{22} \end{pmatrix} \\ &= \begin{pmatrix} \mathfrak{R}_{v1} c_{11} & \mathfrak{R}_{v1} c_{12} \\ \mathfrak{R}_{v2} c_{21} & \mathfrak{R}_{v2} c_{22} \end{pmatrix} \end{aligned}$$

The reproduction number is the dominant eigenvalue of  $K$ .

## Appendix 2

We restrict calculations in the main text to  $n = 2$  because analytical expressions become unwieldy for  $n > 2$  and some impossible for  $n > 4$  and because graphing numerical solutions as functions of sub-population-specific quantities is difficult when  $n > 2$ . Most importantly, however, we doubt that any new ideas emerge when  $n > 2$ . When  $n = 3$ , for example, the next generation matrix is

$$K_3 = \begin{bmatrix} \mathfrak{R}_{v1} c_{11} & \mathfrak{R}_{v1} c_{12} & \mathfrak{R}_{v1} c_{13} \\ \mathfrak{R}_{v2} c_{21} & \mathfrak{R}_{v2} c_{22} & \mathfrak{R}_{v2} c_{23} \\ \mathfrak{R}_{v3} c_{31} & \mathfrak{R}_{v3} c_{32} & \mathfrak{R}_{v3} c_{33} \end{bmatrix}.$$

The characteristic equation is

$$\lambda^3 - \text{Tr}(K_3)\lambda^2 + q\lambda - \det(K_3) = 0,$$

where

$$q = \mathfrak{R}_{v1} c_{11} \mathfrak{R}_{v2} c_{22} + \mathfrak{R}_{v1} c_{11} \mathfrak{R}_{v3} c_{33} + \mathfrak{R}_{v2} c_{22} \mathfrak{R}_{v3} c_{33} - \mathfrak{R}_{v1} c_{12} \mathfrak{R}_{v2} c_{21} - \mathfrak{R}_{v1} c_{13} \mathfrak{R}_{v3} c_{31} - \mathfrak{R}_{v2} c_{23} \mathfrak{R}_{v3} c_{32}.$$

And  $\mathfrak{R}_v$  is the largest eigenvalue of the characteristic equation.

Consider  $\mathfrak{R}_v$  as a function of  $p_1$ ,  $p_2$  and  $p_3$  with all other parameter values fixed. Figure A1 shows the contour plot of  $\mathfrak{R}_v$  for preferential ( $\bar{\varepsilon} > 0$ , see A) and proportional mixing ( $\bar{\varepsilon} = 0$ , see B). Plot C superimposes plots A and B to illustrate that, when mixing is preferential, higher vaccination coverage would be required to achieve  $\mathfrak{R}_v < 1$ . Figure A2 shows three surfaces, corresponding to  $\varepsilon = 0, 0.4$ , and  $0.8$  (from bottom to top). The rectangular parallelepiped bounded by a red surface within which  $\mathfrak{R}_v < 1$  corresponds to the rectangle when  $n = 2$  in manuscript figures 4.

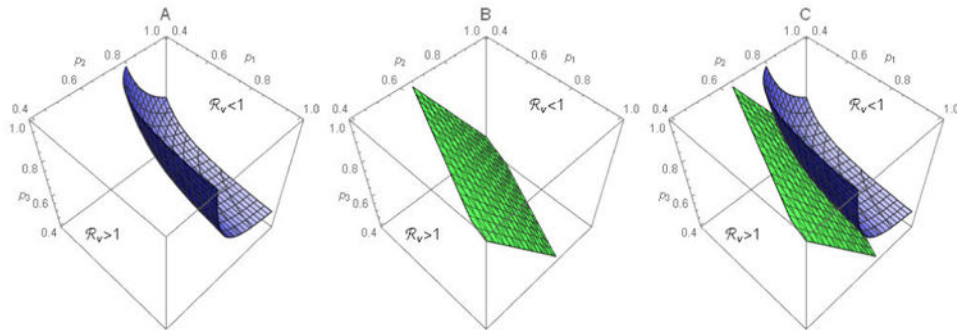


**Figure A1.**

Contour surfaces for 3 sub-groups when mixing is preferential (A) or proportional (B). Plot C superimposes the surfaces in A and B. Parameter values are  $a_1 = 8$ ,  $a_2 = 12$ ,  $a_3 = 10$ ,  $N_1 = N_2 = N_3 = 500$ , and  $\varepsilon_1 = \varepsilon_2 = \varepsilon_3 = \varepsilon$  with  $\varepsilon = 0.4$  in A and  $\varepsilon = 0$  in B.



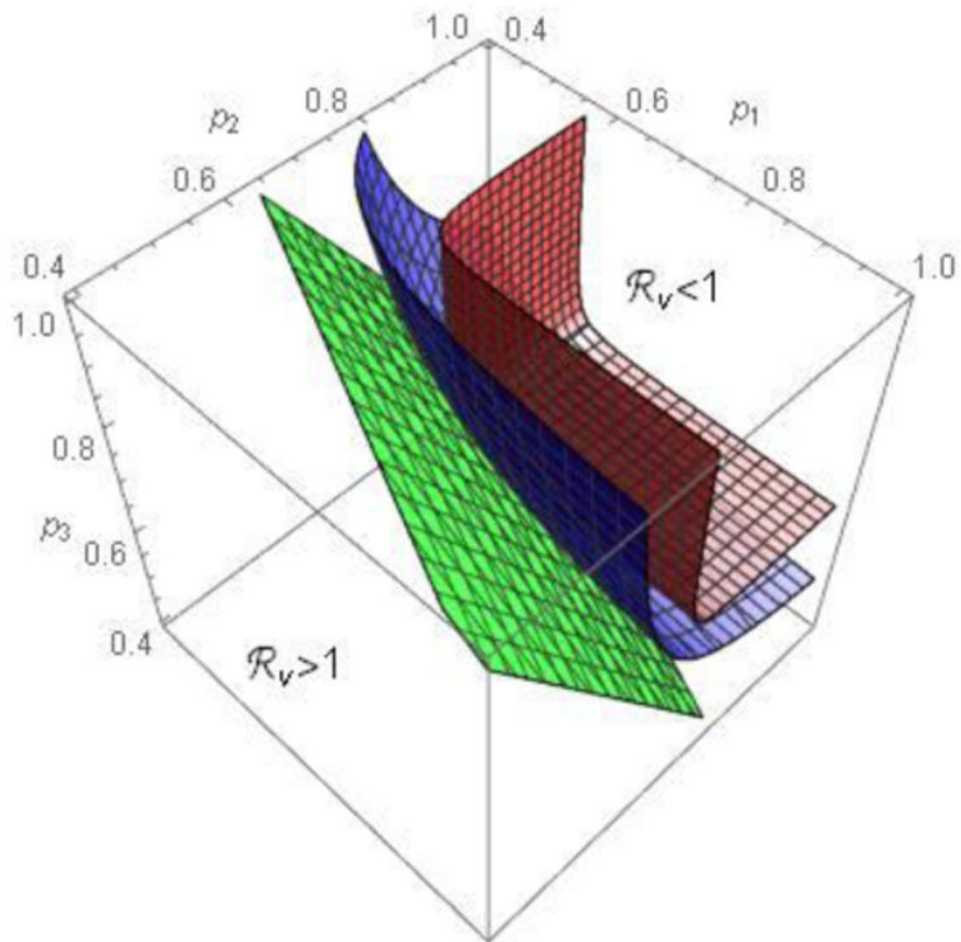


**Figure A2.** Contour surfaces for 3 sub-populations. The surfaces are for  $\bar{\varepsilon} = 0$  (bottom),  $\bar{\varepsilon} = 0.4$  (middle) and  $\bar{\varepsilon} = 0.8$  (top). Other parameter values are the same as in Figure A1.

### Appendix 3

To prove (i), notice that when  $\varepsilon_1 = \varepsilon_2 = 0$ , we have

$$c_{11} = c_{21} = \frac{a_1 N_1}{a_1 N_1 + a_2 N_2} = \frac{a_1}{a_1 + a_2}, \quad c_{22} = c_{12} = \frac{a_2 N_2}{a_1 N_1 + a_2 N_2} = \frac{a_2}{a_1 + a_2}.$$

Thus,

$$R_0 = \frac{\beta}{\gamma + \mu} \left( \frac{a_1^2 + a_2^2}{a_1 + a_2} \right).$$

Let  $a_2 = a_T - a_1$  and let

$$F(a_1) = \frac{a_1^2 + a_2^2}{a_T} = \frac{a_1^2 + (a_T - a_1)^2}{a_T}.$$

Then  $\mathfrak{R}_0 = F(a_1)\beta/(\gamma + \mu)$ . Note that  $F(a_1)$  is a decreasing (increasing) function on  $0 < a_1 < a_T$  ( $a_T/2 < a_1 < a_T$ ) and that  $F(0) = F(a_T)$ . That is,  $F(a_1)$  has a minimum at  $a_1 = a_T/2$ , and it achieves its maximum at  $a_1 = 0$  and  $a_1 = a_T$ . Therefore,  $\mathfrak{R}_0(0,0)$  is minimized when  $a_1 = a_2$ , and maximized when  $a_1 = 0$  and  $a_1 = a_T$ .

To prove (ii), notice that for  $\varepsilon_1 = 1$  or  $\varepsilon_2 = 1$  we have  $c_{11} = c_{22} = 1$  and  $c_{12} = c_{21} = 0$ . Therefore,  $\mathfrak{R}_0(\varepsilon_1, 1) = \mathfrak{R}_0(1, \varepsilon_2) = \max\{\mathfrak{R}_{01}, \mathfrak{R}_{02}\}$ . It is easy to see that  $\max\{\mathfrak{R}_{01}, \mathfrak{R}_{02}\}$  is the smallest when  $a_1 = a_2 = a_T/2$ , and the largest when  $a_1 = 0$  (in which case  $\mathfrak{R}_0 = \mathfrak{R}_{02} = \beta a_T/(\gamma + \mu)$ ) or when  $a_1 = a_T$  (in which case  $\mathfrak{R}_0 = \mathfrak{R}_{01} = \beta a_T/(\gamma + \mu)$ ).

Together with the fact that  $\mathfrak{R}_0(\varepsilon_1, \varepsilon_2)$  increases with  $\varepsilon_1$  and  $\varepsilon_2$  for all  $0 < \varepsilon_1, \varepsilon_2 < 1$ , we would expect the behavior shown in figure 2 (i.e., the  $\mathfrak{R}_0(\varepsilon_1, \varepsilon_2)$  surface moves up as heterogeneity in  $a$  increases).

## References

1. Levins R. Some demographic and genetic consequences of environmental heterogeneity for biological control. *Bulletin of the Entomological Society of America*. 1969; 15(3):237–40.
2. Ball F, Britton T, House T, et al. Seven challenges for meta-population models of epidemics, including household models. *Epidemics*. 2014; doi: 10.1016/j.epidem.2014.08.001
3. Dietz, K. Models for vector-borne parasitic diseases. In: Barigozzi, Claudio, editor. Vito Volterra Symposium on Mathematical Models in Biology Lecture Notes in Biomathematics. Vol. 39. 1980. p. 264–77.
4. Anderson RM, Medley GF, May RM, et al. A preliminary study of the transmission dynamics of human immunodeficiency virus (HIV), the causative agent of AIDS. *IMA J Math Appl Med Biol*. 1986; 3(4):229–63. [PubMed: 3453839]
5. May RM, Anderson RM. The transmission dynamics of human immunodeficiency virus (HIV). *Phil Trans R Soc Lond B*. 1988; 321(1207):565–607. [PubMed: 2907158]
6. Diekmann O, Heesterbeek JAP, Metz JAJ. On the definition and the computation of the basic reproduction ratio  $\mathfrak{R}_0$  in models for infectious diseases in heterogeneous populations. *J Math Biol*. 1990; 28(4):365–82. [PubMed: 2117040]
7. Nold A. Heterogeneity in disease transmission modeling. *Math Biosci*. 1980; 52(3-4):227–40.
8. Jacquez JA, Simon CP, Koopman J, et al. Modeling and analyzing HIV transmission: the effect of contact patterns. *Math Biosci*. 1988; 92(2):119–99.
9. Barbour AD. Macdonald's model and the transmission of bilharzias. *Trans R Soc Trop Med Hyg*. 1978; 72(1):6–15. [PubMed: 635979]
10. Dye C, Hasibeder G. Population dynamics of mosquito-borne disease: effects of flies which bite some people more frequently than others. *Trans R Soc Trop Med Hyg*. 1986; 80(1):69–77. [PubMed: 3727001]
11. Hasibeder G, Dye C. Population dynamics of a mosquito-borne disease: persistence in a completely heterogeneous environment. *Theor Popul Biol*. 1988; 33(1):31–53. [PubMed: 2897726]
12. Adler FR. The effects of averaging on the basic reproduction ratio. *Math Biosci*. 1992; 111(1):89–98. [PubMed: 1515741]
13. May RM, Anderson RM. Spatial heterogeneity and the design of immunization programs. *Math Biosci*. 1984; 72(1):83–111.

14. May RM, Anderson RM. Spatial, temporal and genetic heterogeneity in host populations and the design of immunization programmes. *IMA J Math Appl Math Biol.* 1984; 1(3):233–66.
15. Hethcote HW. An immunization model for a heterogeneous population. *Theor Popul Biol.* 1978; 14(3):338–49. [PubMed: 751264]
16. Hethcote HW, van Ark JW. Epidemiological models for heterogeneous populations: proportionate mixing, parameter estimation and immunization programs. *Math Biosci.* 1987; 84(1):85–118.
17. Fine P, Eames K, Heymann DL. “Herd Immunity”: a rough guide. *Clin Infect Dis.* 2011; 52(7): 911–16. [PubMed: 21427399]
18. Goldstein E, Paur K, Fraser C, Kenah E, Wallinga J, Lipsitch M. Reproductive numbers, epidemic spread and control in a community of households. *Math Biosci.* 2009; 221:11–25. [PubMed: 19559715]
19. van den Driessche P, Watmough J. Reproduction numbers and sub-threshold endemic equilibria for compartmental models of disease transmission. *Math Biosci.* 2002; 180(1-2):29–48. [PubMed: 12387915]
20. Diekmann O, Heesterbeek JAP, Roberts MG. The construction of next-generation matrices for compartmental epidemic models. *J R Soc Interface.* 2010; 7(47):873–85. [PubMed: 19892718]
21. Chow L, Fan M, Feng Z. Dynamics of a multi-group epidemiological model with group-targeted vaccination strategies. *J Theor Biol.* 2011; 291:56–64. [PubMed: 21945582]
22. Colizza V, Vespignani A. Epidemic modeling in metapopulation systems with heterogeneous coupling pattern: theory and simulations. *J Theor Biol.* 2008; 251:450–67. [PubMed: 18222487]
23. Apolloni A, Poletto C, Ramasco JJ, Jensen P, Colizza V. Metapopulation epidemic models with heterogeneous mixing and travel behavior. *Theor Biol Med Model.* 2014; 11:3.doi: 10.1186/1742-4682-11-3 [PubMed: 24418011]
24. Keeling, MJ., Rohani, P. *Modeling Infectious Diseases in Humans and Animals.* Princeton Univ Press; 2007.
25. Goldstein E, Apolloni A, Lewis B, et al. Distribution of vaccine/antivirals and the ‘least spread line’ in a stratified population. *J R Soc Interface.* 2010; 7:755–64. [PubMed: 19828505]
26. Del Valle SY, Hyman JM, Hethcote HW, et al. Mixing patterns between age groups in social networks. *Soc Networks.* 2007; 29(4):539–54.
27. Mossong J, Hens N, Jit M, et al. Social contacts and mixing patterns relevant to the spread of infectious diseases. *PLoS Med.* 2008; 5(3):381–91.
28. Zagheni E, Billari FC, Manfredi P, et al. Using time-use data to parameterize models for the spread of close-contact infectious diseases. *Am J Epidemiol.* 2008; 168(9):1082–90. [PubMed: 18801889]
29. Medlock J, Galvani AP. Optimizing influenza vaccine distribution. *Science.* 2009; 325(5948): 1705–08. [PubMed: 19696313]

## Glossary

$S_i, I_i, R_i, N_i$	Numbers susceptible; numbers infected/infectious; numbers recovered/immune; total number in group (or sub-population) $i$
$\mu, \gamma$	Specific (or <i>per capita</i> ) birth/death and recovery rates
$\lambda_i$	Force (or hazard rate) of infection per susceptible member of group (or sub-population) $i$ , a function defined in the text
$n$	Number of groups (or sub-populations), indexed by $i, j$ , or $k$

$a_i, \beta$	Activity (average <i>per capita</i> contact rate) of people in group $i$ ; probability of infection, if susceptible, upon contact with an infectious person
$c_{ij}$	Mixing (or proportion of the contacts of members of group $i$ that are with members of group $j$ ), a function defined in the text
$I_j/N_j$	Probability that a proportionally contacted member of group $j$ is infected/infectious
$f_j$	Proportional (or activity-weighted proportional) mixing, a function defined in the text
$\varepsilon_i$	Preference (average fraction of contacts reserved for others in one's own group)
$\delta_{ij}$	Kronecker delta, equal to 1 when $i = j$ and 0 otherwise
$\forall i, \exists j$	For all groups $i$ , there is a group $j$
$\mathcal{R}_0, \mathcal{R}_{0i}, \mathcal{R}_v, \mathcal{R}_{vi}$	Overall and group-specific intrinsic (or basic) reproduction numbers, functions defined in the text; Overall and group-specific effective (or control by vaccination, hence the subscript $v$ ) reproduction numbers, functions defined in the text
$p_i, p_c$	Proportion of group $i$ that has been immunized (proportion vaccinated $\times$ vaccine efficacy), proportion immunized at which $\mathcal{R}_v = 1$
$A, B, C, D$	Symbols defined in the text solely to simplify notation
$\mathcal{R}_0$	Average of $\mathcal{R}_{0i}$
$m, \sigma^2$	Mean and variance of $a_i$
$\mathcal{R}_0 / \varepsilon_i, \mathcal{R}_v / p_i$	Partial derivatives of the basic reproduction number with respect to preference and the control reproduction number with respect to immunity
$\nabla \mathcal{R}_v$	Gradient, a vector function defined in the text
$ \nabla \mathcal{R}_v $	Magnitude of the gradient

### Highlights

- Population-immunity thresholds are useful only in homogeneous, proportionally-mixing populations
- Meta-population effective reproduction numbers,  $\mathfrak{R}_v$ , and related quantities always are useful
- Heterogeneity in variables affecting sub-population reproduction numbers is relevant
- Together with preferential mixing among sub-populations, such heterogeneity increases  $\mathfrak{R}_v$
- The vector of partial derivatives of  $\mathfrak{R}_v$  with respect to sub-population immunities indicates which sub-populations to vaccinate to reduce  $\mathfrak{R}_v$  most effectively and efficiently

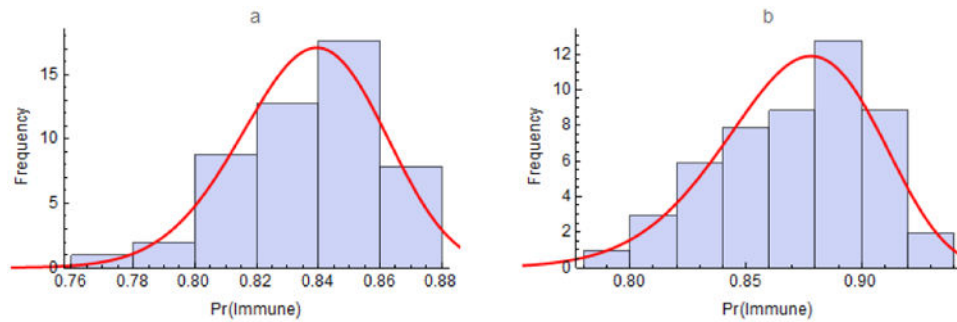


**Figure 1.** Immunity to measles in the United States among a) children aged 19 to 35 months and b) adolescents aged 13 to 17 years for all 50 states and the District of Columbia from the 2012 National Immunization Surveys (<http://www.cdc.gov/vaccines/imz-managers/coverage/nis/child/2012-released.html>). Immunity was estimated as proportions of children with at least one and adolescents with two or more doses of MMR vaccine times efficacies of 92% and 95%, respectively. The curves are fitted beta distributions having shape parameters  $\alpha = 208.39$  and  $\beta = 40.65$  for children and  $\alpha = 83.98$  and  $\beta = 12.52$  for adolescents. Insofar as some adolescents have had one dose of MMR, figure 1b under-estimates their immunity to measles.

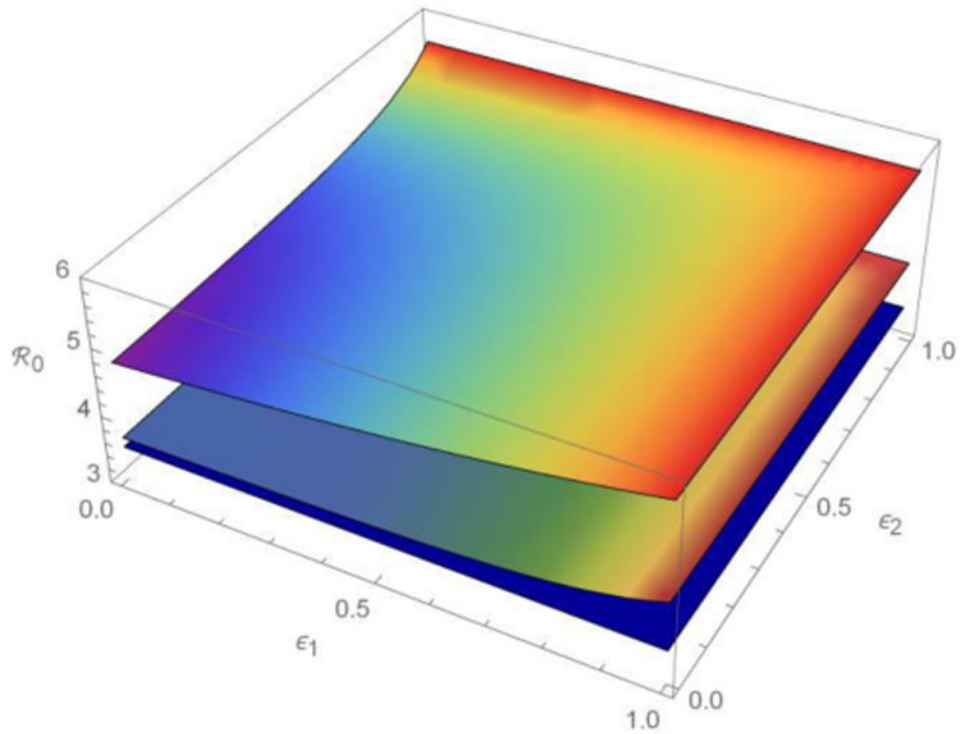


**Figure 2.** The meta-population  $\mathcal{R}_0$  as a function of fractions of the contacts that members of two sub-populations reserve for others within their own sub-populations ( $\epsilon_1, \epsilon_2$ ) when their activities (average contact rates) are more or less heterogeneous.  $\mathcal{R}_0$  decreases from the top surface ( $a_1 = 4, a_2 = 16$ ), through the middle ( $a_1 = 8, a_2 = 12$ ), to the bottom ( $a_1 = a_2 = 10$ ). See table 1 for other parameter values. As heterogeneity in  $\epsilon$  (e.g., ratio of the variance and mean) increases away from the line  $\epsilon_1 = \epsilon_2$ , heterogeneous preferential mixing also increases  $\mathcal{R}_0$ .



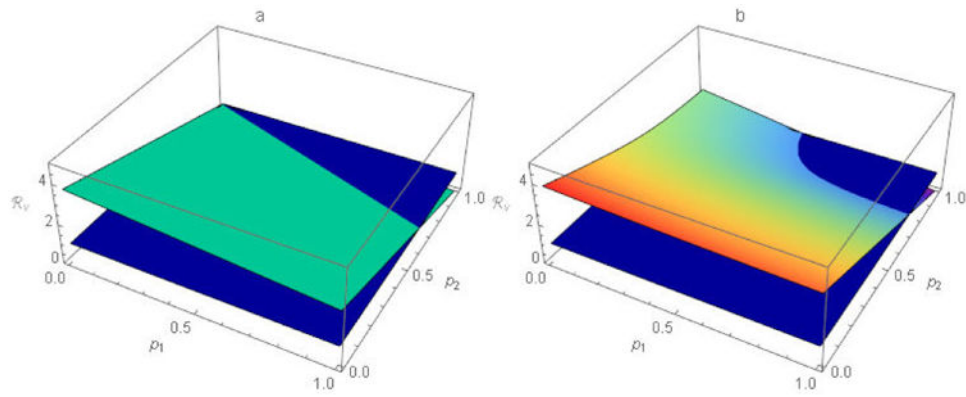


**Figure 3.**

The function  $\mathfrak{R}_v$  for scenario B of table 1 with a) proportional, and b) preferential, mixing. The dark blue planes represent  $\mathfrak{R}_v = 1$  and the lighter blue plane and curved (rainbow) surface represent  $\mathfrak{R}_v$  for other tabulated parameters at all possible  $(p_1, p_2)$  pairs when a)  $\varepsilon_1 = \varepsilon_2 = 0$  and b)  $\varepsilon_1 = \varepsilon_2 = 0.5$ , respectively.  $\mathfrak{R}_v \geq 1$  for all combinations of  $p_i (i=1, 2)$  at or below the dark blue plane. While there is no single population-immunity threshold when  $n > 1$ ,  $\mathfrak{R}_v$  retains its utility as a threshold for outbreak prevention and, ultimately, disease elimination.

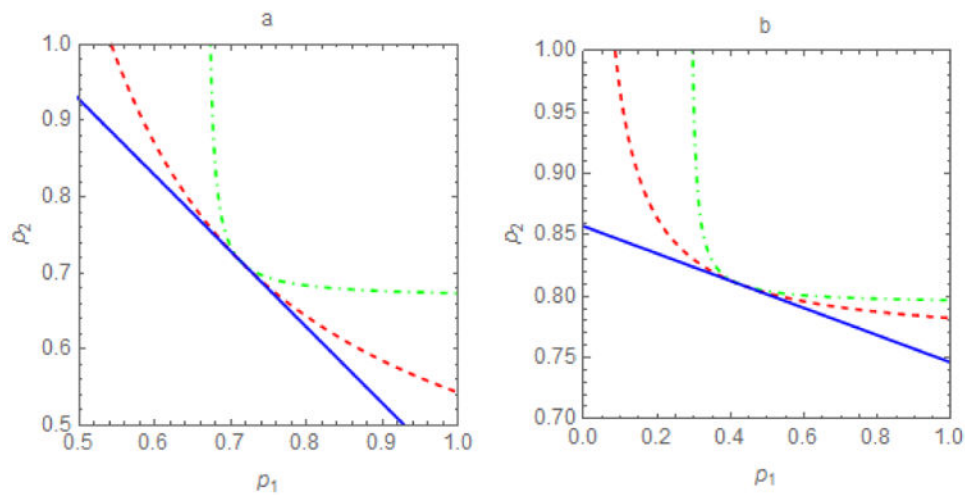


**Figure 4.** Contour plots of the threshold  $\mathcal{R}_v = 1$  in the  $p_1$ - $p_2$  plane for different *per capita* contact rates,  $a$ , and proportions within-group,  $\varepsilon$ . For proportional mixing ( $\varepsilon = 0$ ), the threshold pairs  $(p_1, p_2)$  for outbreak prevention or control form a (dark blue) line,  $p_2 = -bp_1 + r$ , where  $r > 0$  is a constant and  $b=1$  when a) sub-populations are identical in characteristics affecting  $\mathcal{R}_0$  (here  $a_1 = a_2 = 10$ ) and b)  $b \neq 1$  when they differ (here  $a_1 = 5, a_2 = 15$ ). At the other extreme, isolated sub-populations ( $\varepsilon = 1$ ), the region in which  $\mathcal{R}_v < 1$  is a rectangle. In between, dashed curves represent selected  $0 < \varepsilon < 1$  (red,  $\varepsilon_1 = \varepsilon_2 = 0.5$ ; green,  $\varepsilon_1 = \varepsilon_2 = 0.75$ ). These thresholds divide the plane into sub-regions such that  $\mathcal{R}_v > 1$  ( $\mathcal{R}_v < 1$ ) below (above) the line or curve. Preferential mixing increases the difficulty of achieving  $\mathcal{R}_v = 1$ . When  $\varepsilon = 1$ , pairs  $(p_1, p_2)$  must be within a relatively small rectangular area in the upper right quadrant. When  $\varepsilon = 0$ , pairs  $(p_1, p_2)$  need only be in the larger area above the solid line.

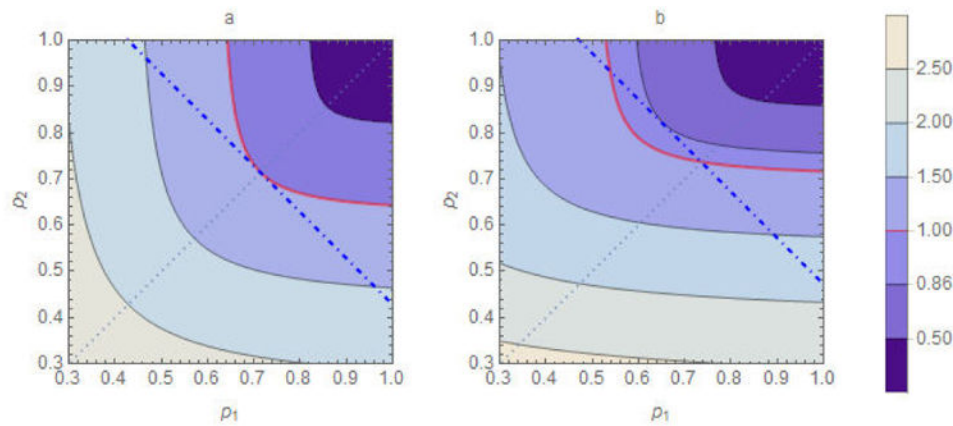


**Figure 5.**

Comparison of homogeneous ( $p_1 = p_2$ ) and heterogeneous immunity ( $p_1 \neq p_2$ ) when mixing is preferential ( $0 < \varepsilon_1, \varepsilon_2 \leq 1$ ). The parameter values are  $\beta = 0.05$ ,  $\gamma = 1/7$ ,  $\varepsilon_1 = \varepsilon_2 = 0.6$ , and  $N_1 = N_2 = 500$ . In figure a),  $a_1 = a_2 = 10$ , in which case  $\mathcal{R}_0 = 3.5$ . The solid curves are contours of the function  $\mathcal{R}_v(p_1, p_2)$  with the thicker (red) curve corresponding to  $\mathcal{R}_v = 1$ . The lighter (dotted)  $p_2 = p_1$  line indicates homogeneous coverage; its intersections with the contour curves represent corresponding  $\mathcal{R}_v$  values. The homogeneous coverage required to achieve  $\mathcal{R}_v = 1$  is  $p_1 = p_2 = 1 - 1/\mathcal{R}_0 = 0.71$ . The thicker dot-dashed line passing through point  $(p_1, p_2) = (0.71, 0.71)$  identifies all  $(p_1, p_2)$  pairs requiring the same number of vaccine doses in sub-populations of the same size (i.e., they satisfy  $p_1 + p_2 = 2 \times 0.71$ ). Its intersections with the contour curves also represent corresponding  $\mathcal{R}_v$  values. Note that  $\mathcal{R}_v > 1$  for all  $(p_1, p_2)$  pairs other than  $(0.71, 0.71)$ . In figure b), where  $a_1 = 8$ ,  $a_2 = 12$ , in which case  $\mathcal{R}_0 = 3.8$ . The homogeneous coverage required to achieve  $\mathcal{R}_v = 1$  is  $p_1 = p_2 = 1 - 1/\mathcal{R}_0 = 0.74$ . We observe some pairs with  $p_1 < 0.74$  for which  $\mathcal{R}_v < 1$ , for one of which  $\mathcal{R}_v = 0.86$ .

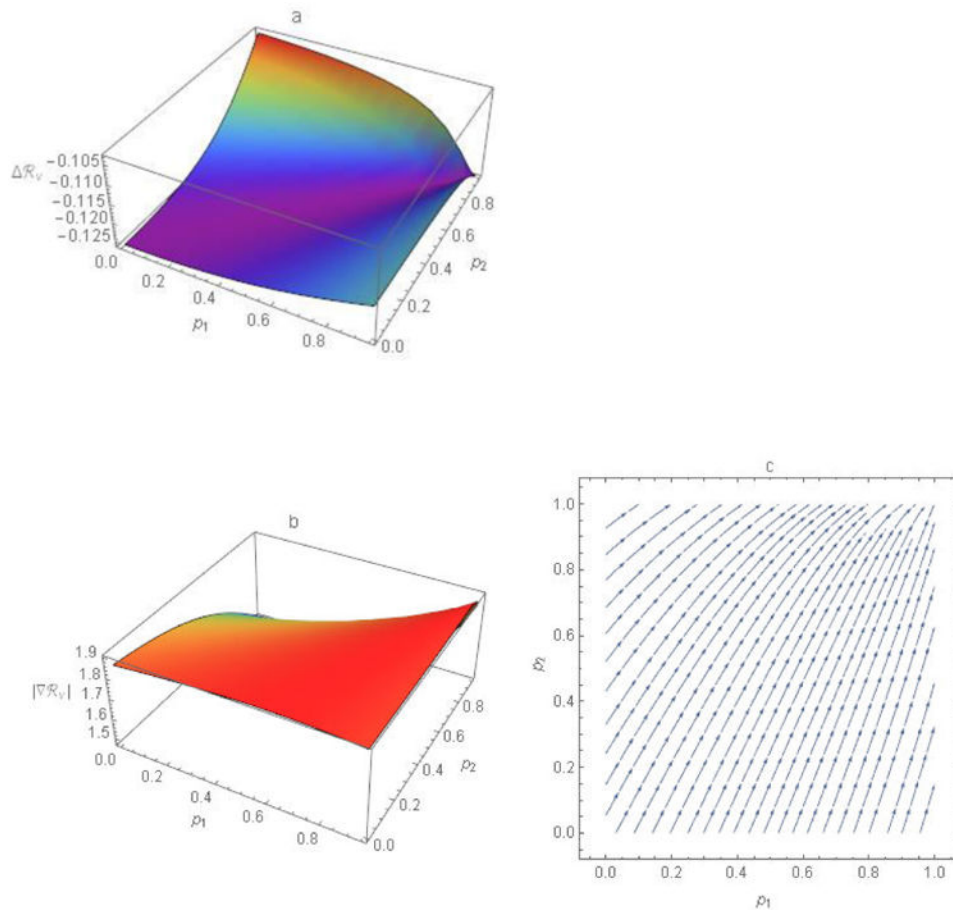


**Figure 6.**

The gradient, the  $n$  partial derivatives of  $\mathcal{R}_v$  with respect to the  $p$ -variables, and the magnitude and direction of this vector-valued function. a) The ASR  $\mathcal{R}_v$  approximates the change in  $\mathcal{R}_v$  at points  $(p_1, p_2)$  corresponding to increases in  $p_1$  and  $p_2$ , here both equal to 0.05. The more negative the value of  $\mathcal{R}_v$ , the larger the reduction. b) Lengths,  $|\nabla \mathcal{R}_v|$ , or magnitudes of the gradient (i.e., rates of change in  $\mathcal{R}_v$ ) at points  $(p_1, p_2)$ . c) Directions of the negative gradient  $\nabla \mathcal{R}_v$  at evenly spaced points  $(p_1, p_2)$  where arrows indicate the changes in  $p_1$  and  $p_2$  that would yield the greatest reductions in  $\mathcal{R}_v$ . Equivalently, at any point  $(p_1, p_2)$ , increasing  $p_1$  and  $p_2$  in the direction of  $\nabla \mathcal{R}_v$  would most efficiently (i.e., require the fewest doses of vaccine) achieve any particular  $\mathcal{R}_v$ . See the text for derivation. Other parameter values are  $\varepsilon_1 = 0.3$ ,  $\varepsilon_2 = 0.1$ ,  $a_1 = 5$ ,  $a_2 = 10$ ,  $N_1 = 750$ , and  $N_2 = 250$ .

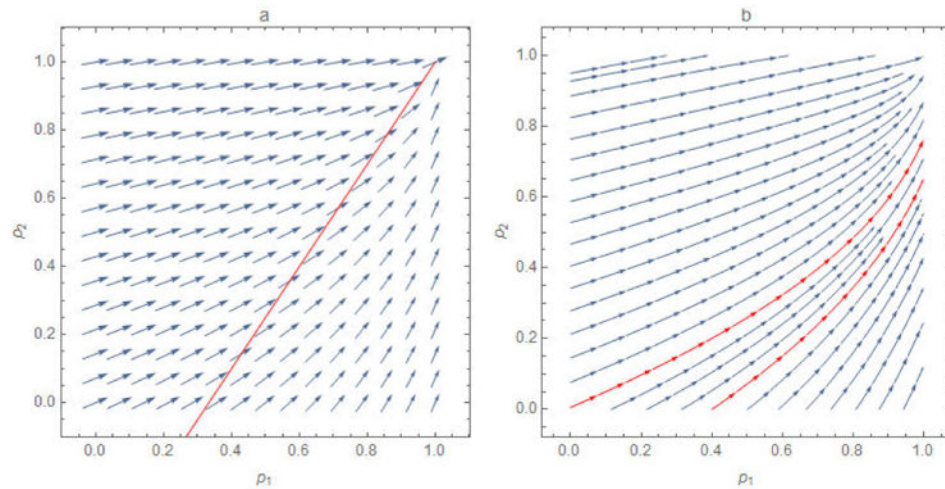


**Figure 7.**

The a) negative gradient  $\nabla \mathcal{R}$  at evenly spaced points  $(p_1, p_2)$  and b) optimal path from arbitrary starting points for a modification of the example of Fine et al. solely to increase transparency. The arrows in figure 7a, a vector plot, indicate the changes in  $p_1$  and  $p_2$  that would yield the greatest reductions in  $\mathcal{R}_v$ , represented by their sizes, while those in figure 7b, a stream plot, indicate only direction. Because these two sub-populations are not isolated, the gradient is defined over the entire parameter space. And, because their contact rates are not as disparate as those of Fine et al., the gradient directions do not seem to be either horizontal or vertical.

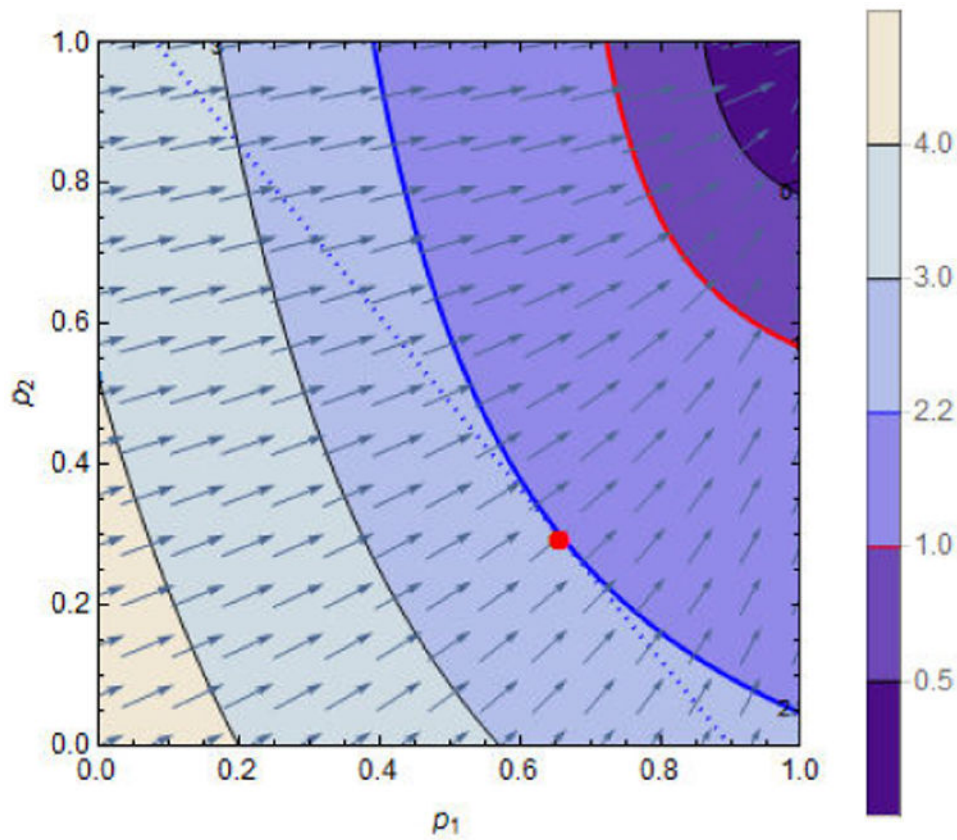


**Figure 8.**

A numerical solution to the Lagrange problem. We observe that the line  $p_2 = (c - p_1 N_1)/N_2$  (dotted) is tangent only to the contour curve  $\mathfrak{R}_v(p_1, p_2) = 2.2$ . They intersect at the point  $(p_1, p_2) = (0.66, 0.29)$ , the optimal solution (marked with a red dot). The parameter  $c = 0.9 \times N_1$  with others the same as in figure 7. For some parameter values, the optimal solution might be outside the unit square in the  $p_1$ - $p_2$  plane.

**Table 1**

Preferential Mixing Magnifies the Impact of Heterogeneity in Person-to-Person Contact Rates (activity) on  $\mathfrak{R}_0$ . The number of sub-populations and their sizes also affect these results, but here  $n = 2$ ,  $N_1 = 500$  and  $N_2 = 500$ , so that the mean activity is the same in scenarios A and B. Common parameters:  $\beta = 0.05$ ,  $\gamma = 1/7$ , and  $N_1 = N_2 = 500$  unless otherwise specified in figure or table legends.

Parameter	Scenario A		Scenario B	
	$a_1 = 10$	$a_2 = 10$	$a_1 = 7.5$	$a_2 = 12.5$
$\mathfrak{R}_{0i}$	3.5	3.5	2.62	4.37
$\mathfrak{R}_0 (\epsilon_1 = \epsilon_2 = 0)$	3.5		3.72	
$\mathfrak{R}_0 (\epsilon_1 = \epsilon_2 = 0.5)$	3.5		3.88	
$\mathfrak{R}_0 (\epsilon_1 = 0.25, \epsilon_2 = 0.75)$	3.5		3.92	
$\mathfrak{R}_0 (\epsilon_1 = 0.75, \epsilon_2 = 0.25)$	3.5		3.98	



**Table 2**

Sub-Population Sizes Affect the Impact of Heterogeneity in Activity and Preferential Mixing on  $\mathfrak{R}_0$ . When sub-population sizes are unequal, as in scenario C, the larger dominates, but when they are equal, as in scenario D, heterogeneity and preferential mixing have greater impact. Other parameters:  $N = 1000$ ,  $a_1 = 5$  and  $a_2 = 10$  (the village and city if  $N_1 \ll N_2$ ).

Parameter	Scenario C		Scenario D	
	$N_1 = 0.1N$	$N_2 = 0.9N$	$N_1 = 0.5N$	$N_2 = 0.5N$
$\mathfrak{R}_{0i}$	1.75	3.5	1.75	3.5
$\mathfrak{R}_0 (\epsilon_1 = \epsilon_2 = 0)$	3.41		2.92	
$\mathfrak{R}_0 (\epsilon_1 = \epsilon_2 = 0.5)$	3.44		3.09	
$\mathfrak{R}_0 (\epsilon_1 = 0.25, \epsilon_2 = 0.75)$	3.42		3.12	
$\mathfrak{R}_0 (\epsilon_1 = 0.75, \epsilon_2 = 0.25)$	3.46		3.2	